ARTICLES

Adaptation to the Edge of Chaos with Random-Wavelet Feedback

Timothy Wotherspoon* and Alfred Hübler

Center for Complex Systems Research, Physics Department, University of Illinois at Urbana–Champaign, 1110 West Green Street, Urbana, Illinois 61801

Received: May 19, 2008; Revised Manuscript Received: August 27, 2008

We studied the effect of low-pass band filters on the dynamics of a nonisothermal autocatalator as seen through feedback on a system parameter. Filters were created by selecting Fourier coefficients for the modes in the pass band according to a uniform distribution. Numerical simulations over many realizations of feedback were compared to theoretical predictions for the feedback size as a function of the parameter. We found that the variance in the feedback was nonzero only near and within chaotic regimes in the parameter space. We numerically calculated the probability density for the parameter, showing that the system adapts to the edge of chaos.

1. Introduction

There has been much interest lately in the wealth of behavior possible in open chemical reactions. This includes such behaviors as oscillating pH structures,[1] Turing and other patterns,[2−5] symmetry breaking,[6] and pattern concatenation.[7] Another possibility in open chemical reactions is the presence of chaotic dynamics. Chaotic oscillations were first observed in the Belousov–Zhabotinskii reaction in the 1970s.[8] Since then, chaotic dynamics have been observed in heterogeneous catalysis reactions,[9] electrodissolution reactions,[10] and biochemical systems.[11] These observations have hence brought great interest to the topic of how to control chaos in a chemical reaction.[12−16] In fact, so much has been written on the topic of chaotic chemical reactions and how to control them that one might be led to believe that chaotic dynamics is quite common in open chemical reactions. This is, in fact, not the case. Chaotic dynamics is indeed rare.

Because of the nonlinear nature of most chemical reactions and the presence of feedback through autocatalysis and/or self-heating, one would expect chaotic dynamics to be abundant in chemical reactions. However, as mentioned, only a small portion of reactions exhibit chaotic behavior. One is thus left wondering: why the apparent lack of chaos in chemistry? Previous studies have investigated the effect of a low-pass-filtered feedback from a dynamical variable to the control parameter on the logistic map[17] and the Chua circuit.[18] It was found that the low-pass filter resulted in the systems adapting to a state at the boundary of chaos and order known as the edge of chaos. We examined numerical simulations of a nonisothermal autocatalator in the presence of a similar low-pass filter.

We found that the presence of a low-pass-filtered feedback in a nonisothermal autocatalator results in the system evolving to the edge of chaos. Low-pass filters are believed to be quite common in nature, particularly in dissipative chemical reactions. These results thus suggest that such naturally occurring low-pass filters might be one reason for the apparent scarcity of chaotic dynamics in open chemical reactions.

* To whom correspondence should be addressed. E-mail: wothersp@uiuc.edu.

2. Random-Wavelet Feedback

To model feedback in chemical reactions, we first start with a model of the reaction. Typically, this is a set of coupled nonlinear differential equations with J observables, x_j, and K parameters, μ_k, so that

$$\dot{x}_j = f(\{x_j\},\{\mu_k\}) \tag{1}$$

To apply feedback, we take the natural dynamics $x[t,(\mu_k)]$, for t going from 0 to T and a parameter μ and apply the map

$$\mu_{n+1} = \mu_n + \varepsilon F(\mu_n) \tag{2}$$

where ε is a small number such that $|\varepsilon F| \ll |\mu|$ and $F(t)$ is the filter output defined as

$$F(T,\mu) = (1/T)\int_0^T x(t,\mu)\, g(t)\, \mathrm{d}t \tag{3}$$

The function $g(t)$ is our random wavelet, defined as

$$g(t) = \sum_{n_i}^{n_f} \left[u_n \cos\left(\frac{\pi n t}{T}\right) + v_n \sin\left(\frac{\pi n t}{T}\right)\right] \tag{4}$$

where u_n and v_n are independent random numbers from a distribution ρ. This is a band-pass filter with frequency cutoffs at $f_{low} = n_i/2T$ and $f_{high} = n_f/2T$. It is important that the time, T, be much greater than the relevant time scales in the natural dynamics. This assures a separation of time scales between the parameter dynamics and the natural dynamics of the system and neglects any transient effects. The dynamics of the parameter are overdamped motion with no attractor, even for a given realization of filter values. Because the parameter is fixed over short time scales, the dynamical variables behave as if there is no coupling between them and the control parameters.

To examine the expected result of the feedback, the first step is to express the signal, $x(t)$, in terms of its harmonics

10.1021/jp804420g CCC: $40.75 © 2009 American Chemical Society
Published on Web 12/15/2008

$$x(t) = \frac{b_0}{2} + \sum_{n=1}^{\infty}\left[a_n \sin\left(\frac{\pi n t}{T}\right) + b_n \cos\left(\frac{\pi n t}{T}\right)\right] \quad (5)$$

where

$$a_n = \frac{1}{T}\int_0^T x(t) \sin\left(\frac{\pi n t}{T}\right) \mathrm{d}t \quad (6)$$

$$b_n = \frac{1}{T}\int_0^T x(t) \cos\left(\frac{\pi n t}{T}\right) \mathrm{d}t \quad (7)$$

In this way, the filter output can be expressed as

$$F(T,\mu) = \sum_{n_i}^{n_f} u_n a_n + v_n b_n \quad (8)$$

To determine where the system will adapt, it is useful to know the size and variance of the filter output. To do this, we must integrate each of these random variables over the distribution in the following way

$$\bar{F} = \int \left(\sum_{n_i}^{n_f} u_n a_n + v_n b_n\right) \rho(u_{n_i}) \cdots \rho(u_{n_f})\, \rho(v_{n_i}) \cdots \rho(v_{n_f})\, \mathrm{d}u_{n_i} \cdots \mathrm{d}u_{n_f} \mathrm{d}v_{n_i} \cdots \mathrm{d}v_{n_f} \quad (9)$$

which simplifies to

$$\bar{F} = \sum_{n_i}^{n_f}\left[a_n \int u_n \rho(u_n)\, \mathrm{d}u_n + b_n \int v_n \rho(v_n)\, \mathrm{d}v_n\right] \quad (10)$$

$$= \sum_{n_i}^{n_f} (a_n \overline{u_\mathrm{n}} + b_n \overline{v_\mathrm{n}}) \quad (11)$$

Thus, the mean filter output will be 0 if the mean of the distribution ρ is 0. In that case, the mean is 0 for any signal. The signal is much more important when calculating the variance of the filter output. Assuming that the filter output has a mean of 0, the variance is given by

$$\sigma_{F(\mu)}^{\;2} = \int \left(\sum_{n_i}^{n_f} u_n a_n + v_n b_n\right)^2 \rho(u_{n_i}) \cdots \rho(u_{n_f})\, \rho(v_{n_i}) \cdots \rho(v_{n_f})\, \mathrm{d}u_{n_i} \cdots \mathrm{d}u_{n_f} \mathrm{d}v_{n_i} \cdots \mathrm{d}v_{n_f} \quad (12)$$

which we expand to

$$\sigma_{F(\mu)}^{\;2} = \int \left[\sum_{n_i}^{n_f} (u_n^{\;2} a_n^{\;2} + v_n^{\;2} b_n^{\;2}) + \sum_{j \neq k} (u_j u_k a_j a_k + v_j v_k b_j b_k)\right] \rho(u_{n_i}) \cdots \rho(u_{n_f})\, \rho(v_{n_i}) \cdots \rho(v_{n_f})\, \mathrm{d}u_{n_i} \cdots \mathrm{d}u_{n_f} \mathrm{d}v_{n_i} \cdots \mathrm{d}v_{n_f} \quad (13)$$

Each term in the second sum is linear in an integrand, so these terms will integrate to 0 as in the caluclation of the mean, so that we can further simplify the variance to

$$\sigma_{F(\mu)}^{\;2} = \sum_{n_i}^{n_f}\left[a_n^{\;2} \int u_n^{\;2} \rho(u_n)\, \mathrm{d}u_n + b_n^{\;2} \int v_n^{\;2} \rho(v_n)\, \mathrm{d}v_n\right] \quad (14)$$

$$= \sum_{n_i}^{n_f} a_n^{\;2} \overline{u_n^{\;2}} + b_n^{\;2} \overline{v_n^{\;2}} \quad (15)$$

It is natural to choose the same distribution for each term in the sum, so in practice

$$\sigma_{F(\mu)}^{\;2} = \sum_{n_i}^{n_f} \overline{u^2} S_n^{\;2} \quad (16)$$

where

$$S_n^{\;2} = a_n^{\;2} + b_n^{\;2} \quad (17)$$

is the power series of the natural dynamics.

This result is important because it suggests the band over which filtering should take place. Figure 2 (below) is typical for a chaotic system. The behavior in the lowest frequencies is sensitive to the sampling of the data. In principal, the theory works whenever the sum goes over frequencies that are not present in the periodic dynamics. Chaotic parameter values have dynamics with contributions in all modes. Thus, the window that we chose is not unique; it is simply the easiest one to find.

3. Non-Isothermal Autocatalators

For an example, we numerically studied a model for nonisothermal autocatalators that describes reactions of the type[19]

$$\mathrm{P} \rightarrow \mathrm{A}$$
$$\mathrm{A} \rightarrow \mathrm{B}$$
$$\mathrm{A} + 2\mathrm{B} \rightarrow 3\mathrm{B}$$
$$\mathrm{B} \rightarrow \mathrm{C} + \text{heat}$$

This reaction was modeled by the following set of nonlinear ordinary differential equations on dimensionless variables

$$\frac{\mathrm{d}\alpha}{\mathrm{d}\tau} = \mu \mathrm{e}^{\theta} - \alpha\beta^2 - \kappa_\mathrm{u}\alpha \quad (18)$$

$$\frac{\mathrm{d}\beta}{\mathrm{d}\tau} = \alpha\beta^2 + \kappa_\mathrm{u}\alpha - \beta \quad (19)$$

$$\frac{\mathrm{d}\theta}{\mathrm{d}\tau} = \delta\beta - \gamma\theta \quad (20)$$

where α and β are the dimensionless concentrations of A and B, respectively; θ is the difference between the reaction temperature and the ambient temperature; and τ is the time. The parameters δ and γ serve, respectively, as measures of the exothermicity of the fourth step in the reaction and the surface heat-transfer coefficient. Finally, κ_u is a rate coefficient. For all of our simulations, we used $\delta = 0.1$, $\gamma = 0.5$, and $\kappa_\mathrm{u} = 0.0055$, with initial conditions $\alpha(0) = 0.8$, $\beta(0) = 0.6$, and $\theta(0) = 1.0$.

The final parameter, μ, is the initial concentration of reactant P. This parameter determines much for the dynamics of the system. Figure 1 shows a bifurcation diagram of the dynamics of the system. For $0.65 < \mu < 0.688$, all dynamical variables, i.e., α, β, and θ, undergo a period doubling sequence. For $0.689 < \mu < 0.696$, the dynamics is mostly chaotic, although there do exist several small periodic windows within this range. For $0.696 < \mu < 0.7$, the dynamics is once again periodic. The edge of chaos refers to values of μ for which a small perturbation would take the system from periodic dynamics to chaotic dynamics or from chaotic dynamics to periodic dynamics. Values of μ that are very near 0.689 or 0.696 or that are within the periodic windows are thus at the edge of chaos. To apply the feedback described above, we coupled μ to the temperature difference θ. The choice of μ also determines the behavior of the power series for the dynamics. Figure 2 shows the power series $S(f)$, where $f = n/2T$, in θ for four different parameter values. This choice of coupling creates a model for a reactor that slowly self-adjusts its initial concentration of reactant according to the filter output. It is not within the scope of this article to suggest how such a feedback mechanism could occur

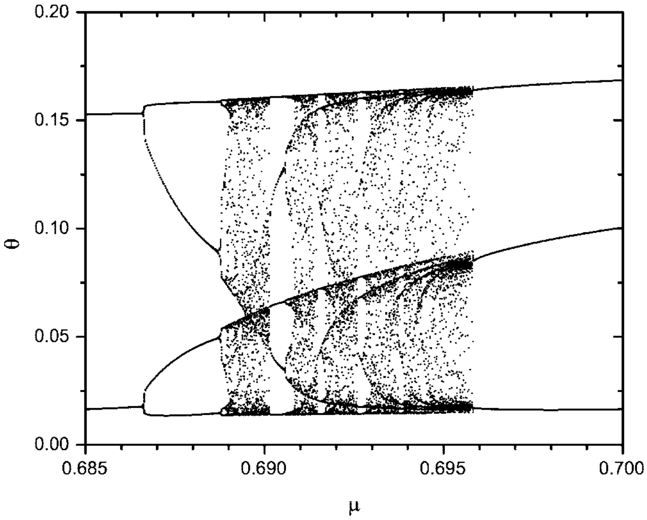

Figure 1. Local minima in the dynamics of the variable θ as a function of the parameter μ, showing a period-doubling road to chaos and providing a picture of the behavior of the dynamics throughout our parameter range. Similar figures could be drawn for α and β.

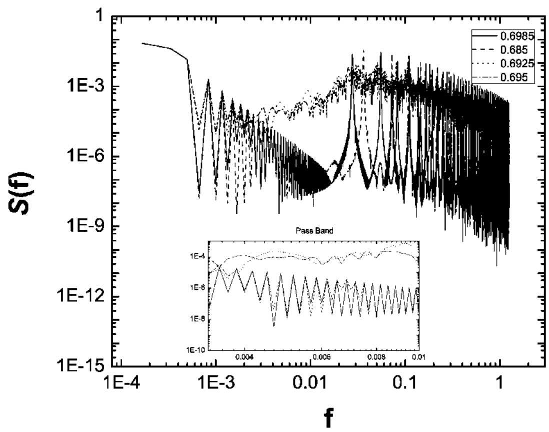

Figure 2. Power-series data for four parameter values in the chemical system as a function of frequency. The filter used pass modes between $f = 0.0067$ and $f = 0.02$. In this band, chaotic parameter values have power-series values that are orders of magnitude greater than the power-series values for periodic parameter values.

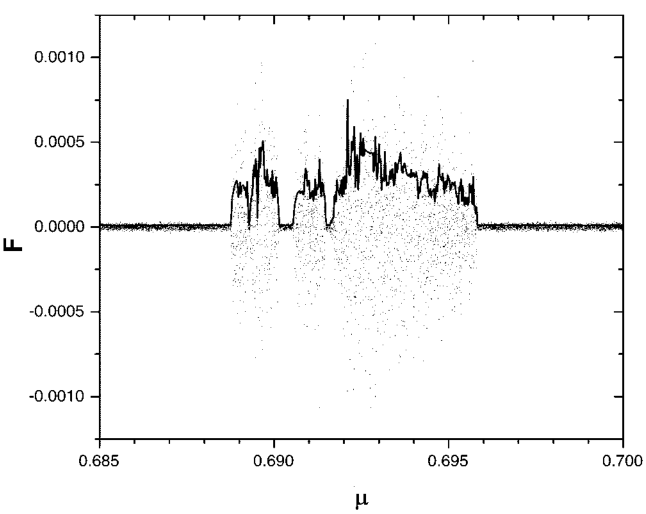

Figure 3. Ten realizations of the random-wavelet feedback (points) and predictions for the variance according to eq 14 (line). Chaotic values of the parameter give much stronger feedback.

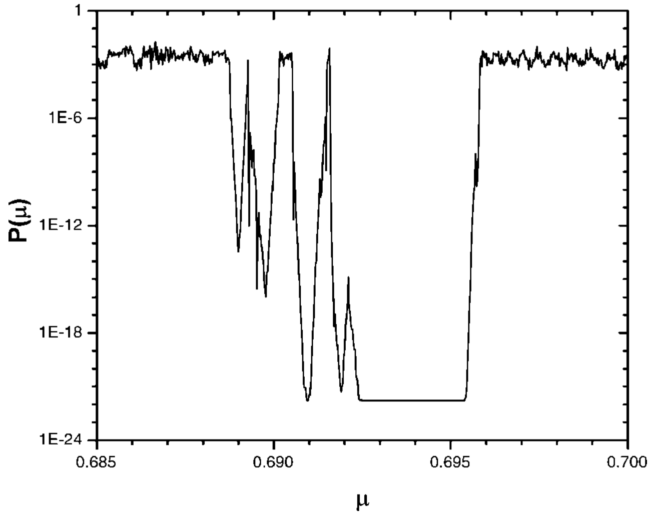

Figure 4. Twenty iterations of Euler's method on the master equation. The probability becomes several orders of magnitude smaller in the chaotic regions than in the periodic regions, showing adaptation to the edge of chaos.

naturally, only that the details of the feedback mechanism are not important. In a laboratory, one possible implementation of such a system could be investigated by manually adjusting the concentration of the initial reactant after the reaction has been running for a prescribed time T.

Figure 3 shows the filter output for 10 filter realizations, as well as the predicted result for the variance from eq 14. In our work, we ran 10 000 realizations and found that the spread was in excellent agreement. This is unsurprising. The filtering calculates the same Fourier coefficients that we must calculate in order to make a prediction. Such a comparison tests that our random-number generator gives the appropriate mean and spread.

4. Probability Density

We can use these data to numerically calculate the probability density for the parameter. If we consider the dynamics of the parameter, from Figure 3, we expect an random walk through the parameter space. However, in the chaotic regions, the average step size is much larger than the step size in the periodic regions. To see how the probability density behaves in time, we begin with a master equation description of the system

$$\dot{P}(\mu) = \sum_{\mu' \neq \mu} P(\mu')\, w(\mu',\mu) - P(\mu) \sum_{\mu' \neq \mu} w(\mu,\mu') \qquad (21)$$

where $w(\mu', \mu)$ is the transition probability from μ' to μ. From eq 2, we obtain

$$w(\mu',\mu) = P(\varepsilon F) \qquad (22)$$

One needs to know how the filter output is distributed in order to determine the transition probabilities. Inspection of histograms of the filter output shows that it is distributed normally, so that

$$w(\mu',\mu) = \frac{1}{\sqrt{2\pi\sigma_{F(\mu')}{}^2}} \frac{\Delta\mu}{\varepsilon} \exp\left[-\frac{(\mu'-\mu)^2}{2\varepsilon^2 \sigma_{F(\mu')}{}^2}\right] \qquad (23)$$

where $\Delta\mu$ is the parameter spacing. For analytical results, one must express $\mu' - \mu$ in terms of $\Delta\mu$ and take the limit as $\Delta\mu \rightarrow 0$.

Because the parameter dynamics is discrete in time, we numerically integrate eq 21 with Euler's method. Rewriting eq 21 as

$$P_{n+1}(\mu) - P_n(\mu) = \sum_{\mu' \neq \mu} P_n(\mu')\, w(\mu',\mu) - P_n(\mu) \sum_{\mu' \neq \mu} w(\mu,\mu') \tag{24}$$

with

$$\sum_{\mu' \neq \mu} w(\mu,\mu') = 1 - w(\mu,\mu) \tag{25}$$

we obtain

$$P_{n+1}(\mu) = \sum_{\mu'} P_n(\mu')\, w(\mu',\mu) \tag{26}$$

Thus, the behavior of the probability density can be observed with matrix multiplication. Figure 4 shows 20 iterations of this map. Here, $\Delta\mu = 2.5 \times 10^{-5}$ and $\varepsilon = 0.1$. For this value of ε, $\varepsilon\sigma_F/\Delta\mu$ is on the order of unity for values of σ_F in the chaotic regime. Starting with an initially flat distribution, it can be seen that the chaotic regime becomes quickly unpopulated. This shows adaptation to the edge of chaos for this system.

5. Conclusion

Finally, we find according to eq 14 that the size of feedback depends on the Fourier components of the time series. Given an appropriate pass band, such as the one inset in Figure 2, we conclude that all filters with this pass band give large feedback in the chaotic regime of the parameter space when compared to feedback in the periodic regime, independent of the Fourier coefficients of the filter, as seen in Figure 3. This causes the probability density for the parameter value to be small in the chaotic regime and large in the periodic regimes. Thus, this system exhibits adaptation to the edge of chaos.

Acknowledgment. This work builds upon an unpublished undergraduate research project by Alex Barr. The work was supported by NSF DMR 03-25939.

References and Notes

(1) Li, G.; Ouyang, Q.; Swinney, H. L. *J. Chem. Phys.* **1996**, *105*, 10830.
(2) Ouyang, Q.; Li, R.; Li, G.; Swinney, H. L. *J. Chem. Phys.* **1995**, *102*, 2551.
(3) Lee, K. J.; McCormick, W. D.; Swinney, H. L.; Noszticzius, Z. *J. Chem. Phys.* **1992**, *96*, 4048.
(4) Vastano, J. A.; Pearson, J. E.; Horsthemke, W.; Swinney, H. L. *J. Chem. Phys.* **1988**, *88*, 6175.
(5) Tam, W. Y.; Horsthemke, W.; Noszticzius, Z.; Swinney, H. L. *J. Chem. Phys.* **1988**, *88*, 3395.
(6) Kreisberg, N.; McCormick, W. D.; Swinney, H. L. *J. Chem. Phys.* **1989**, *91*, 6532.
(7) Mase Ko, J.; Swinney, H. L. *J. Chem. Phys.* **1986**, *85*, 6430.
(8) Schmitz, R.; Graziani, K.; Hudson, J. *J. Chem. Phys.* **1977**, *67*, 7.
(9) Carabineiro, S.; Van Noort, W.; Nieuwenhuys, B. *Surf. Sci.* **2003**, *532*, 96.
(10) Li, W.; Nobe, K.; Pearlstein, J. *J. Electrochem. Soc.* **1993**, *140*, 721.
(11) Olsen, L.; Degn, H. *Nature* **1977**, *267*, 177.
(12) Gong, J.; Brumer, P. *J. Chem. Phys.* **2001**, *115*, 3590.
(13) Fujisaki, H.; Takatsuka, K. *J. Chem. Phys.* **2001**, *114*, 3497.
(14) Baier, G.; Sahle, S.; Chen, J.-P.; Hoff, A. A. *J. Chem. Phys.* **1999**, *110*, 3251.
(15) Baier, G.; Sahle, S. *J. Chem. Phys.* **1994**, *100*, 8907.
(16) Petrov, V.; Peng, B.; Showalter, K. *J. Chem. Phys.* **1992**, *96*, 7506.
(17) Melby, P.; Kaidel, J.; Weber, N.; Hübler, A. *Phys. Rev. Lett.* **2000**, *84*, 5991.
(18) Melby, P.; Weber, N.; Hübler, A. *Fluct. Noise Lett.* **2002**, *2*, 4.
(19) Scott S. K. In *Chemical Chaos*, 1st ed.; Rowlinson, J. S., Ed.; Oxford University Press: New York, 1991; Vol. 1, Chapter 4, p 74.

JP804420G